7-9-2019

Angular Dependence of Third-Order Optical Nonlinearity in Indium Tin Oxide

Bryan J. Crossman
College of Saint Benedict/Saint John's University, bjcrossman@csbsju.edu

Angular Dependence of Third-Order Optical Nonlinearity in Indium Tin Oxide

Bryan Crossman
College of Saint Benedict/Saint John's University
Senior Thesis, 2019

Table of Contents

Abstract *3*

Introduction *4*

Theory *5*

Nonlinear Behavior of ITO **5**

Two-Temperature Model **6**

Simplified Model **6**

Experiment *7*

Ti:sapphire Laser **7**

Pump Probe Spectroscopy **8**

Noise Reduction **9**

Data Collection Program **10**

Angular Dependence Procedure **12**

Electric Field Procedure **10**

Analysis *12*

Cross-Correlation **12**

Maximum Signal Change **12**

Modeling ITO Scans **13**

Gold Scan **13**

Conclusion *14*

Maximum Signal **14**

Decay Times **14**

Comparison to Gold **15**

Final Comments **15**

Bibliography *17*

Figures and Tables *19*

Abstract

The nonlinear optical response of indium tin oxide (ITO) is measured at various pump incident angles using 50-fs, 800-nm laser pulses with a pulse energy of 9 nJ. The temporary ultrafast transmittance changes in the ITO sample are attributed to changes in both the real and imaginary parts of the nonlinear index of refraction. These changes correspond to two third-order nonlinear optical processes, known as self-focusing and saturable absorption, which enhance the transmittance of incident light through the sample. The data we collect is fit using a simplified two-temperature-model. We determine that the change in the transmitted light due to nonlinear optical processes in the ITO increases by a factor of 2.3 as the incident angle is increased from 0 to 60 degrees. The electron-phonon coupling time constant in ITO is measured to be 12 +/- 3 fs. We also compare the nonlinear response of ITO with a similar thickness gold film while holding the incident angle constant. We show that the nonlinear process in thin film gold occurs on a time scale that is almost 20 times longer than in the ITO. These results show promise for the use of ITO in optical devices requiring modulation of the refractive index on an ultrafast time scale.

Introduction

A long-standing goal in optics is to find materials with controllable indices of refraction for implementation in electro-optical devices. Materials with such a property are useful for ultrafast laser pulse generation and optical switching.[1] Using ultrafast laser pulses with sufficiently high peak intensities, it is possible to see large shifts in the index of refraction of conductive materials due to third-order nonlinear processes.[2-6] Recently, experiments concerning the nonlinear optical behavior of indium tin oxide (ITO) have shown that this material has an index of refraction for near-IR wavelengths which can be changed relatively easily.[7-9] ITO is a n-type semiconducting oxide which is transparent through the visible range but reflective in the IR. Due to its interesting electro-optical properties, ITO has been implemented in electronic displays, touch screens, and energy efficient window coatings. Previous research on the nonlinear optical properties of ITO has shown that changes to both the real and imaginary components of the nonlinear index of refraction occur by changing the angle of incident light or by placing the sample in an intense static electric field.[7-9]

Our study adds to the work of Alam et. al since we are conducting a similar experiment.[7] However, the two main differences are the wavelength and pulse duration of our laser system. Laser pulse duration is the main factor that limits the duration of the processes which can be observed using a pump-probe spectroscopy experimental set-up. The previous investigations used pulses with a duration of about 100 fs when observing the ultrafast excitation and relaxation processes in ITO.[7,8] The pulses we use have a duration of 50 fs which results in a cross correlation between the pump and probe pulses of around 90 fs full-width at half-maximum. This allows us to observe ultrafast changes in the transmittance behavior of ITO that are a factor of two faster than those in previous research. Also, by probing the sample with pulses centered at 800 nm, we can observe how the angular dependence of the incident pump pulses changes the

nonlinear optical behavior of ITO in a similar wavelength regime. Previous measurements were taken using wavelengths of 720 to 780 nm and 950 to 1450 nm.[7,8] Our measurements will attempt to further our understanding concerning the nonlinear optical properties of ITO.

Theory

Nonlinear Behavior of ITO

When sufficiently high intensity light is incident on indium-tin-oxide, it exhibits a change in both the real and imaginary components of its nonlinear index of refraction, which causes self-focusing and saturable absorption.[7] The changes in the real and imaginary components of the nonlinear refractive index are proportional to the intensity of the laser pulses with proportionality constants n_2 and β, respectively.[7-8] This leads to a change in the linear index of refraction modeled by the equations $\Delta n_0 = n_2 I$ and $\Delta \alpha = \beta I$, where n_0 is the real component and α is the imaginary component of the linear index of refraction. These constants have been shown to depend on both the wavelength and incident angle of pulses.[7] Experimental values of n_2 and β have been determined for wavelengths of 950 to 1450 nm and with pump incident angles from 0 to 60 degrees by Alam *et al*.[7] Their study shows that the index of refraction change is most substantial around the epsilon near-zero (ENZ) wavelength, at which the real part of the permittivity of ITO approaches zero. This occurs due to the fact that the incident light on the material has a frequency that is similar to the plasma frequency in the material.[7] We hope to investigate if there is a similar enhancement of the n_2 and β values at slightly lower wavelengths (785 to 815 nm).

Two-Temperature Model

The nonlinear optical phenomena that occur in thin film conducting metals and semi-conductors can be modeled using the two-temperature model.[4,10-11] A simplified version of this model can be described using the coupled differential equations below:

$$\frac{\partial(C_e T_e)}{\partial t} = -G(T_e - T_l) \quad \text{(Eq. 1)}$$

$$\frac{\partial(C_p T_l)}{\partial t} = G(T_e - T_l) \quad \text{(Eq. 2)}$$

Where G is the value of the electron-phonon interaction coefficient, C_e and C_p are the heat capacities of the electrons and phonons, T_e is the electron temperature, and T_l is the temperature of the lattice.[10] This model assumes that the incoming laser pulse has a delta-function temporal pulse intensity profile with near-zero duration which creates a nonequilibrium condition where the electrons initially are hotter than the lattice.

Simplified Model

We have developed a theoretical model that uses the same assumptions as previous two-temperature models[4,10-11]:

$$D(t_i) = \sum_{j=0}^{i} PU(t_j) exp\left(\frac{-t_i - t_j}{a}\right) \quad \text{(Eq. 3)}$$

$$T(\tau_i) = c_0 + c_1 \sum_{k=0}^{i} PR(t_k) D(t_k + \tau_i) \quad \text{(Eq. 4)}$$

Where the function $D(t)$ corresponds to the total energy that has been deposited by the pump pulse into the sample's conduction electrons and has not yet been transferred to the lattice. $T(\tau)$ is the change in the probe pulse energy transmitted through the ITO sample due to the temporary excitation of the sample. The function $PU(t)$ is the normalized pump pulse power, $PR(t)$ is the

normalized probe pulse power, τ is the time delay between the pulses, c_0 and c_1 are constants corresponding to constant background noise and maximum amplitude of the nonlinear signal, and a is the electron-phonon thermalization time constant. Our model takes two Gaussian pulses, corresponding to the pump and probe pulses, and computes their cross-correlation while accounting for energy transfer through electron phonon-coupling. The underlying assumptions in this model are that the carrier electrons in the conductor do not thermalize with the lattice structure immediately and that energy transfer between electrons and the lattice occurs over a finite time. This model is consistent with what is known about electron-lattice energy transfer behaviors.[4,10-11] If we assume that the excitation of the carrier electrons is nearly instantaneous, then we expect that the initial change in the probe signal will have a similar time scale as in the measured cross-correlation of the pump and probe pulses (i.e. approximately 100 fs). However, the signal should take longer to return to the equilibrium value than the cross-correlation, due to the electron-phonon thermalization time constant. Using this model, we can determine the electron-phonon thermalization time constant for the nonlinear optical processes in ITO thin films.

Experiment

Ti:sapphire Laser

We produce near-infrared laser pulses with duration of around 50 fs using a home-built titanium-doped-sapphire (Ti:sapphire) laser. A Ti:sapphire crystal is pumped with a 4.25-W, 532-nm continuous-wave beam from a commercial laser. The output spectral bandwidth of the Ti:sapphire laser is controlled using an intracavity double-pass fused silica prism pair. The spectrum of the resulting pulses ranges from 785 nm to 815 nm at full-width-half-maximum corresponding to a bandwidth of 30 nm. Although the laser can produce a broader bandwidth,

this relatively smaller bandwidth allows for easier compensation of material dispersion in our experiment and corresponds to a higher output power. The average power of the Ti:sapphire output is 0.8 W with a repetition rate of 86 MHz, corresponding to a 9 nJ pulse energy. A second-harmonic-generation frequency-resolved-optical-gating (SHG FROG) device was used to determine that the duration of both the pump and probe pulses at the location of the sample is around 50 fs at full-width-half-maximum and that these pulses have a nearly Gaussian temporal shape.

Pump Probe Spectroscopy

We use a standard pump-probe setup to examine the nonlinear optical properties of ITO. A diagram of our experimental setup is shown in Fig. 1. The Ti:sapphire output is split into two different beams using a 50/50 beam splitter. An adjustable neutral density filter reduces the probe beam power to be 40 times smaller than the pump beam power. The more energetic pump pulses stimulate the nonlinear interactions that occur in the sample. The probe pulses detect any changes in the amount of light that passes through the sample due to the effects of the incident pump pulses. The pump and probe beams are focused onto the sample using lenses of 15 cm and 20 cm focal length, respectively. This results in a focal spot diameter (measured to $\frac{1}{e^2}$ of the beam's maximum intensity) of 60 μm for the pump beam and 20 μm for the probe beam on the sample surface. The power of the pump and probe beam at the sample surface are 40 mW and 1 mW, respectively. The probe beam fluence (units of $\mathrm{J/cm^2}$) is kept lower than the pump beam fluence (a fluence ratio of around 0.23) to ensure that any observed reduction or increase in the amount of probe light through the sample is only a result of the pump pulses and not due to the probe pulse. Both beam paths involve several lenses and filters which have dispersion that causes

changes in the pulse duration. Thus, two double-pass fused silica prism pairs compensate for this dispersion ensuring that the pulses are sufficiently short at the sample.

To observe the temporal nonlinear effects in ITO, the path length of the probe pulse is modified by a stepper-motor with a connected retro-reflecting mirror. Both paths of the experiment were carefully constructed to ensure they have the same optical pathlength. This means that the pump and probe pulses overlap both spatially and temporally on the surface of the ITO sample. The effects of the pump pulses on the ITO can be measured as a change in the probe light transmitted through the sample by using a silicon photodiode detector. By modifying the probe path length, we can observe time-dependent nonlinear effects in the material with a step size of approximately 5 fs. The cross-correlation of the pump and probe pulses is measured to be around 90 fs at full-width-half-maximum using a beta barium borate (BBO) second harmonic generation crystal. This value gives an idea of the fastest nonlinear optical processes we can observe.

Noise Reduction

There are multiple precautions that are implemented for noise reduction. First, the pump beam is chopped at 25 kHz using an acousto-optical modulator. When the pump beam interacts with the ITO sample surface, the transmitted probe beam will pick up this frequency modulation. Using a lock-in amplifier, we can filter out all light that enters the detector not modulated at this frequency. As another precaution, a half-wave plate and a polarizing filter are placed in the pump path to rotate the polarization of the pump beam by 90 degrees and ensure a pure vertical linear polarization. A second polarizing filter with its transmission axis oriented perpendicular to the transmission axis of the first polarizer is placed in front of the photodiode detector. Therefore, any scattered pump light that may reach the detector will be filtered out. Both of these

precautions help to increase the signal-to-noise ratio of the experiment and ensure that we minimize artifacts from scattered pump light.

Data Collection Program

We wrote a LabVIEW program to automate the data collection process. This program controls the stepper motor and graphically represents the output of the lock-in amplifier as a voltage change versus time delay plot. The stepper motor position is modified to create a time-domain step size of 5 fs between data points on the plot. At each motor position, the program reads the output of the lock-in amplifier 10 times and averages the values. This reduces the noise that results from random fluctuations of the lock-in amplifier signal. The entire scanning process is repeated 20 to 30 times. A single scan takes around one hour to complete. An example of one of these scans is shown in Fig. 2 for ITO at 30-degree incidence angle. We average the first 15 scans that do not show any effects due to temperature fluctuations in the laboratory. Such temperature fluctuations cause the background signal to change continuously over the course of many scans and likely are due to small changes in the alignment of mirrors in the system. These scans where temperature fluctuations occur are disregarded.

Electric Field Procedure

One aspect of our experiment is attempting to see a change in the intensity of the nonlinear signal by applying a static electric field across the ITO film. A diagram of this sample is shown in Fig. 3. We use an ITO film on a PET plastic substrate. The thickness of the ITO is 100 nm, while the PET has a thickness of 0.1 mm. The sample is placed between two 100 nm thickness gold films on glass substrates. The pair of gold films act as parallel plate capacitor when a potential difference is applied across them. With this sample setup, we are limited by the voltage that can be applied across the ITO. The maximum voltage before any sparking occurs

between the two gold samples is 1.3 kV. The corresponding maximum electric field magnitude with these parameters is 10 MV/m, calculated by dividing the applied voltage by the gold plate separation.

The signal that is observed when using this sample is an amalgamation of the nonlinear optical processes that occur in the gold films and the ITO. A pump incident angle of 20 degrees is used during this study to ensure that we have a good overlap between the pump and probe beams. Scans are taken with single gold films to determine how the presence of the gold in the combined sample affects the overall scan. We observe that the overall scans can be created by adding the magnitudes of both the expected gold film and ITO at a given time step. The offset between the beginning of the first gold film signal and the second was calculated to be around 200 fs due to the 0.1 mm distance separating these two films. The signal from the nonlinear optical process in the ITO would occur almost concurrently with the first gold film signal as they are in contact with each other. Scans also are taken with the ITO by itself in the path of the laser. We determine that the excitation and relaxation of the ITO occur on a time interval of around 200 fs. The peak ITO signal is around 30 times smaller than the gold sample when there is no external electric field applied.

Our attempts to find an increase in the nonlinear signal as a result of the applied static electric field did not show an increase in the amount of probe light transmitted through the sample. This is most likely due to the electric field being too weak to show a substantial increase in the nonlinear signal with our sample thickness. We were unsuccessful in finding such an increase in nonlinear signal using a maximum voltage of 1.3 kV and a separation distance of 0.1 mm between the two gold samples.

Angular Dependence Procedure

We also performed scans with a 100-nm-thick ITO sample (Thorlabs part number WTSQ11050-B) on a 5-mm-thick glass substrate to determine the relationship between the peak ITO scan value and the pump beam incident angle. Multiple scans are collected and averaged to determine a single average value for the maximum at each angle. We found that the signal from the ITO increases as the incident angle is increased from 0 to 60 degrees. The experimental setup does not allow for pump incident angles higher than 60 degrees. The trend agrees with other nonlinear optical measurements using ITO.[7]

Analysis

Cross-Correlation

The time length of the nonlinear optical phenomena in this experiment is limited by the cross-correlation of the pump and probe beams. The cross-correlation is a function that specifies the overlap of the pump and probe pulses at the surface of the sample. The pulse width measurements from the FROG are shown in Fig. 4 and Fig. 5. We fit a Gaussian curve to our measurement to show that it is a good representation of the cross-correlation, which is shown in Fig. 6. Our value of full-width-at-half-maximum is around 90 fs for this cross-correlation measurement. This value is half that of previous research on ITO, which allows us to measure optical processes that are twice as fast.

Maximum Signal Change

The maximum value for each averaged scan is used to verify that our system gives data similar to previous investigations of incident angle dependence on the nonlinear ITO signal. These maximum signal values are plotted in Fig. 7. This plot shows that we are seeing similar behavior to that in Alam et. al.[7]; namely, we see that as the pump angle increases, there is an

increase in the maximum signal due to nonlinear optical processes in the material. We determine that the largest nonlinear signal intensity comes at an incident angle of 60 degrees. However, since our experimental set-up was not conducive to incident angles over 60 degrees, we cannot say definitively that this is the maximum value for any incident angle.

Modeling ITO Scans

The bulk of our analysis is done using a Mathematica program that employs Eq. 3 and Eq. 4 to model the scan data. The nonlinear signal was fit to the theoretical model by varying the electron-lattice thermalization time a, and the two constants corresponding to the maximum signal intensity and background signal c_0 and c_1. An example of one fit is shown in Fig. 8, showing the ITO nonlinear response with its corresponding fit at a pump incident angle of 30 degrees. The c_1 constant was determined by taking the difference between the maximum and minimum values of each scan. The fit values for each scan are shown in Table 1. As a measure of fit accuracy, we have computed the reduced-chi-squared value ($\overline{\chi^2}$) for each fit. We attempted to minimize the reduced-chi-squared by adjusting the fit parameters. The models produced for each of the incident pump angles are shown in Fig. 9 with modified c_0 constant values to separate the fits.

Gold Scan

We also have taken scans using a 100 nm thick gold film sample as a comparison to the nonlinear response of the ITO. Fig. 10 shows the scans for the gold film at an incident angle of 30 degrees with its corresponding fit. The fit values are shown in Table 1.

Conclusion

Maximum Signal

ITO shows capabilities as a transparent material with a tunable nonlinear index of refraction based on incident angle. In our data collection, we have shown the change in nonlinear optical behavior with respect to incident pump angle is consistent with the effects described in Alam et. al.[7] However, the increase in the maximum transmission value is not to the same extent as in their study at 950 to 1450 nm. We observe a factor of 2.3 increase in the maximum transmission signal by increasing the incident angle of the pump pulse from 0 to 60 degrees. The one deviation from this trend is the 45-degree value which is approximately equal to the maximum value at 30 degrees. This is most likely due to a problem obtaining an optimal spatial overlap of the pump and probe focal spots. These values are for a center wavelength of 800 nm.

Decay Times

The electron-phonon coupling time constants are fairly consistent at all incident angles. The values for these constants for 0, 15, 30, 45, and 60 degrees are 11, 13, 10, 18, and 9 fs respectively. These values have an average of 12 fs. The estimated uncertainty of these calculated constants is +/- 3 fs. The decay time at 45 degrees is the one outlier in this group. The difference in decay time at this incident angle might be caused by a different optical process that occurs on the back side of the ITO sample. Preliminary scans at all incident angles exhibited this secondary excitation as well, but were corrected by improving the spatial overlap of the pump and probe beams on the ITO surface. Our data agrees with the two-temperature model's assumption that the electron-phonon coupling coefficient is independent of the temperature of the electron. Thus, even if a higher incident angle causes more energy to be deposited into the ITO film, we expect that the decay back to equilibrium will occur at the same rate.

Comparison to Gold

The fact that the gold scan data cannot be fit with our model gives valuable information about the dynamics of its electron-photon interaction. The most notable aspect of this fit is the portion that occurs before zero time delay. We observe that the initial excitation, corresponding to energy transfer from the pump pulse to the carrier electrons, occurs on a time scale that is longer than the rise time of the pump pulse. With the pulse durations used in this experiment, we seem to have surpassed the threshold at which we can assume this initial excitation process is instantaneous—especially in the gold sample. Thus, our two-temperature model needs modification to deal with a slower initial excitation of the electrons in thin film gold. However, the assumption that this process occurs instantaneously in ITO films still appears valid.

Our model still accurately represents the return of the signal to equilibrium, and, thus, gives a reasonable prediction of the electron-phonon coupling time constant in the thin film gold sample. The gold film exhibits an electron-phonon decay time constant of 200 fs ± 5 fs. This value is a factor of around 20 times longer than the electron-phonon coupling time constant of ITO. Thus, the relaxation of the carrier electrons in ITO happens on a much faster time scale than in gold films.

Final Comments

Our experiment highlights the promise that ITO shows as a transparent semi-conductive material for application in electro optical devices. It exhibits a tunable index of refraction change which can be modulated by increasing the incident angle of light on the surface of the material. ITO also shows a much faster electron-phonon coupling time than other conductive thin films such as gold. These properties show that ITO has potential as a material with controllable nonlinear-optical refractive index that can be utilized in systems which require ultrafast modulation of transmittance.

Bibliography

1. Kauranen, Martti, and Anatoly V Zayats. “Nonlinear Plasmonics.” *Nature Photonics*, vol. 6, 31 Oct. 2012, pp. 737–748., doi:10.1038/NPHOTON.2012.244.
2. Ganeev, R A, et al. “Nonlinear Susceptibilities, Absorption Coefficients and Refractive Indices of Colloidal Metals.” *Journal of Physics D: Applied Physics*, vol. 34, no. 11, 2001, pp. 1602–1611., doi:10.1088/0022-3727/34/11/308.
3. Tan, Sherman J. R., et al. “Chemical Stabilization of 1T′ Phase Transition Metal Dichalcogenides with Giant Optical Kerr Nonlinearity.” *Journal of the American Chemical Society*, vol. 139, no. 6, 2017, pp. 2504–2511., doi:10.1021/jacs.6b13238.
4. Brorson, S. D., J. G. Fujimoto, and E. P. Ippen. “Femtosecond Electronic Heat-Transport Dynamics in Thin Gold Films.” *Physical Review Letters* 59, no. 17 (October 26, 1987): 1962–65. doi.org/10.1103/PhysRevLett.59.1962.
5. Fatti, N. Del, and F. Vallée. “Ultrafast Optical Nonlinear Properties of Metal Nanoparticles.” *Applied Physics B: Lasers and Optics*, vol. 73, no. 4, 2001, pp. 383–390., doi:10.1007/s003400100648.
6. Zhou, P., et al. “Linear and Ultrafast Nonlinear Optical Response of Ag:Bi2O3 Composite Films.” *Applied Physics Letters*, vol. 83, no. 19, 2003, pp. 3876–3878., doi:10.1063/1.1626023.
7. Alam, M. Zahirul, Israel De Leon, and Robert W. Boyd. “Large Optical Nonlinearity of Indium Tin Oxide in Its Epsilon-near-Zero Region.” *Science*, April 28, 2016, aae0330. doi.org/10.1126/science.aae0330.

8. Elim, H.i., et al. “Carrier Concentration Dependence of Optical Kerr Nonlinearity in Indium Tin Oxide Films.” *Applied Physics B*, vol. 82, no. 3, 2006, pp. 439–442., doi:10.1007/s00340-005-2079-8.
9. Feigenbaum, Eyal, et al. “Unity-Order Index Change in Transparent Conducting Oxides at Visible Frequencies.” *Nano Letters*, vol. 10, no. 6, 2010, pp. 2111–2116., doi:10.1021/nl1006307.
10. Singh, Navinder. “Two-Temperature Model Of Nonequilibrium Electron Relaxation: A Review.” *International Journal of Modern Physics B*, vol. 24, no. 09, 2010, pp. 1141–1158., doi:10.1142/s0217979210055366.
11. Jiang, Lan, and Hai-Lung Tsai. “Improved Two-Temperature Model and Its Application in Ultrashort Laser Heating of Metal Films.” *Journal of Heat Transfer*, vol. 127, no. 10, Oct. 2005, pp. 1167–1173., doi:10.1115/1.2035113.

Figures and Tables

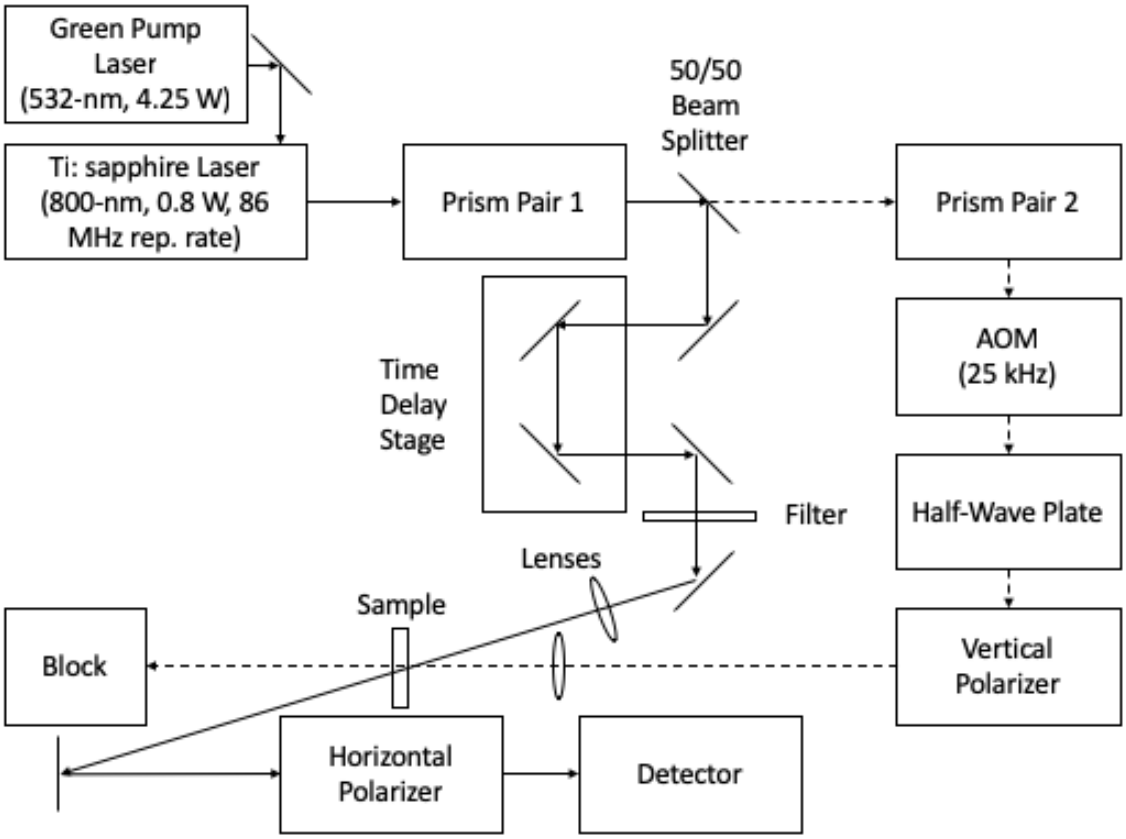

Figure 1. Experimental pump-probe spectroscopy setup: This figure shows both the pump and probe paths of the laser and the optical equipment used to modify the two beams.

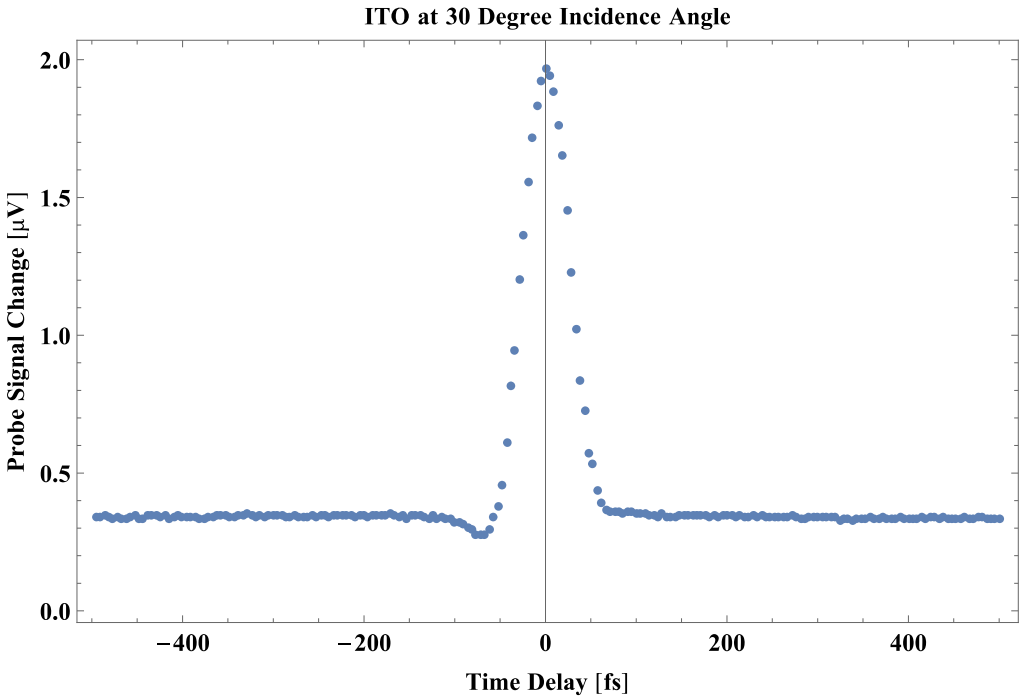

Figure 2. An example of the data collected from the scanning procedure for ITO with a pump incidence angle of 30 degrees

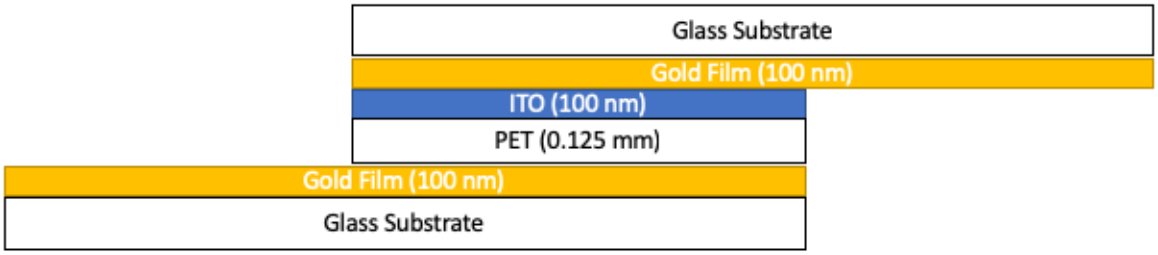

Figure 3. ITO sample diagram with gold films for electric field production

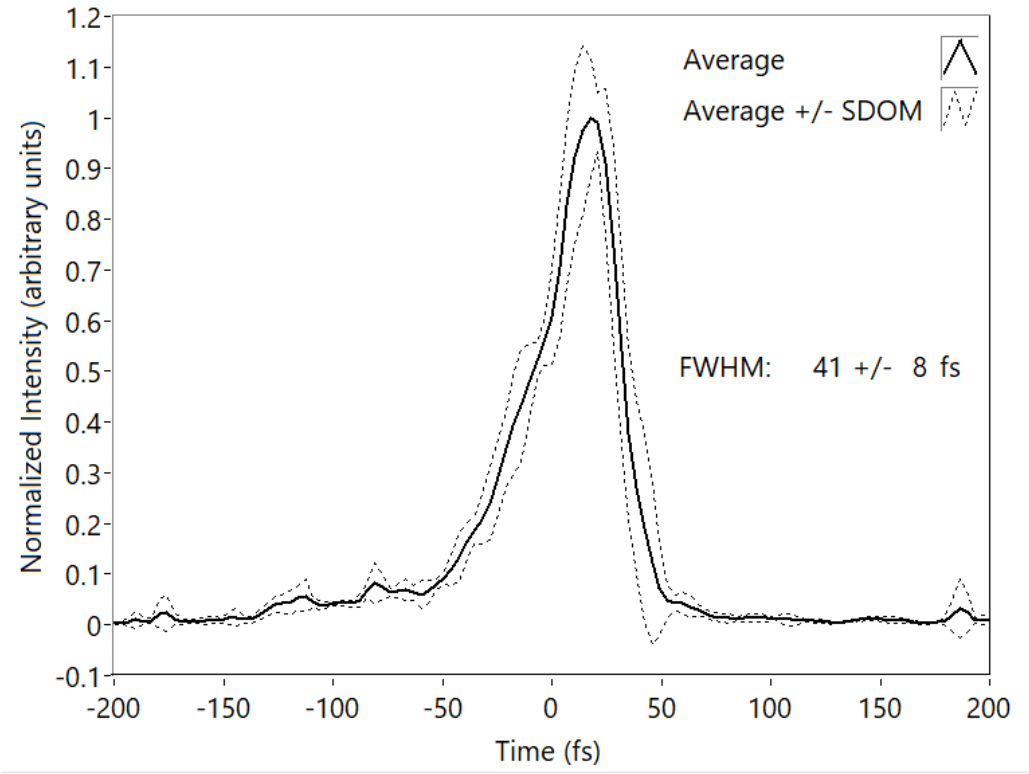

Figure 4. FROG pulse duration measurements for the pump pulses

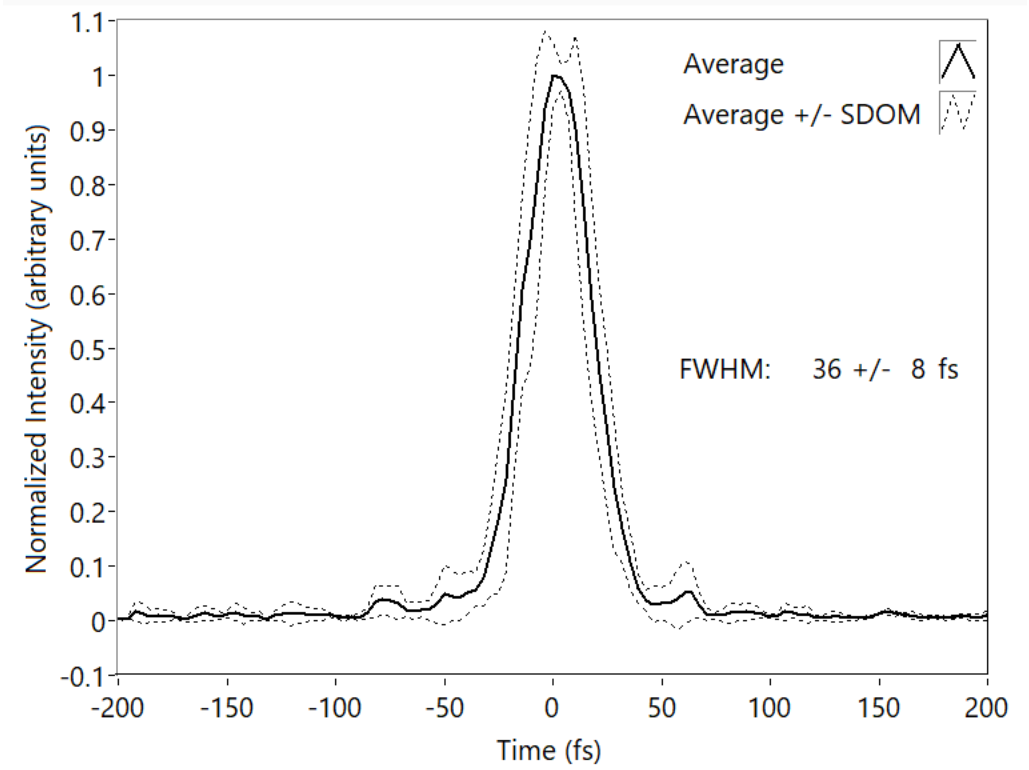

Figure 5. FROG pulse duration measurements for the probe pulses

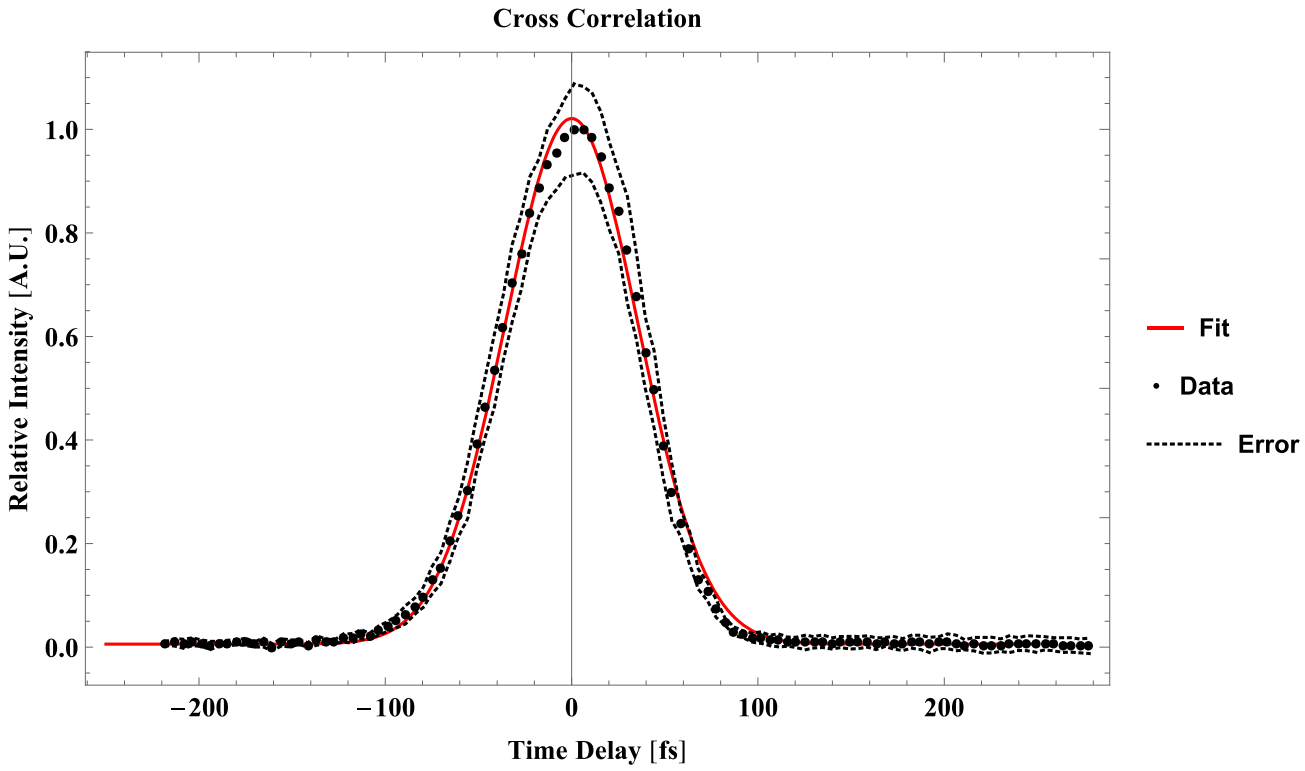

Figure 6. Cross correlation with fit measured using a second harmonic generation BBO crystal

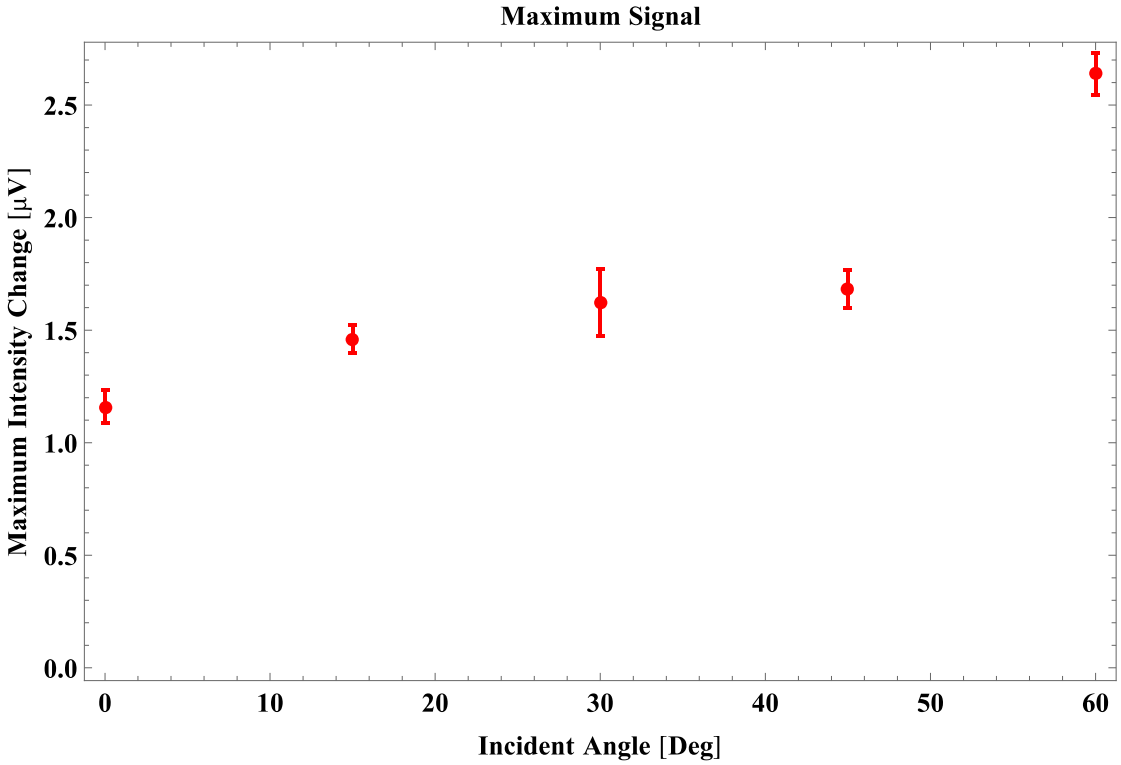

Figure 7. Maximum nonlinear signal intensities for ITO angular dependence survey

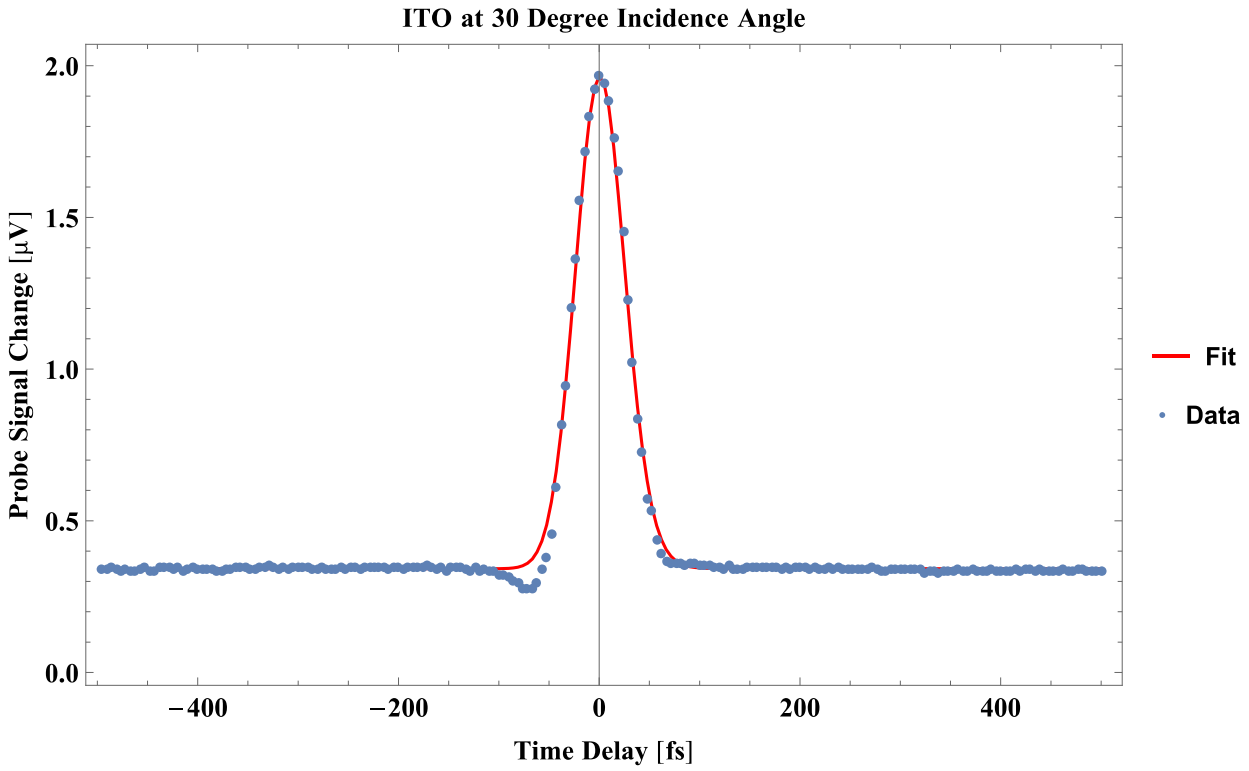

Figure 8. ITO scan with fit for 30-degree pump incidence angle

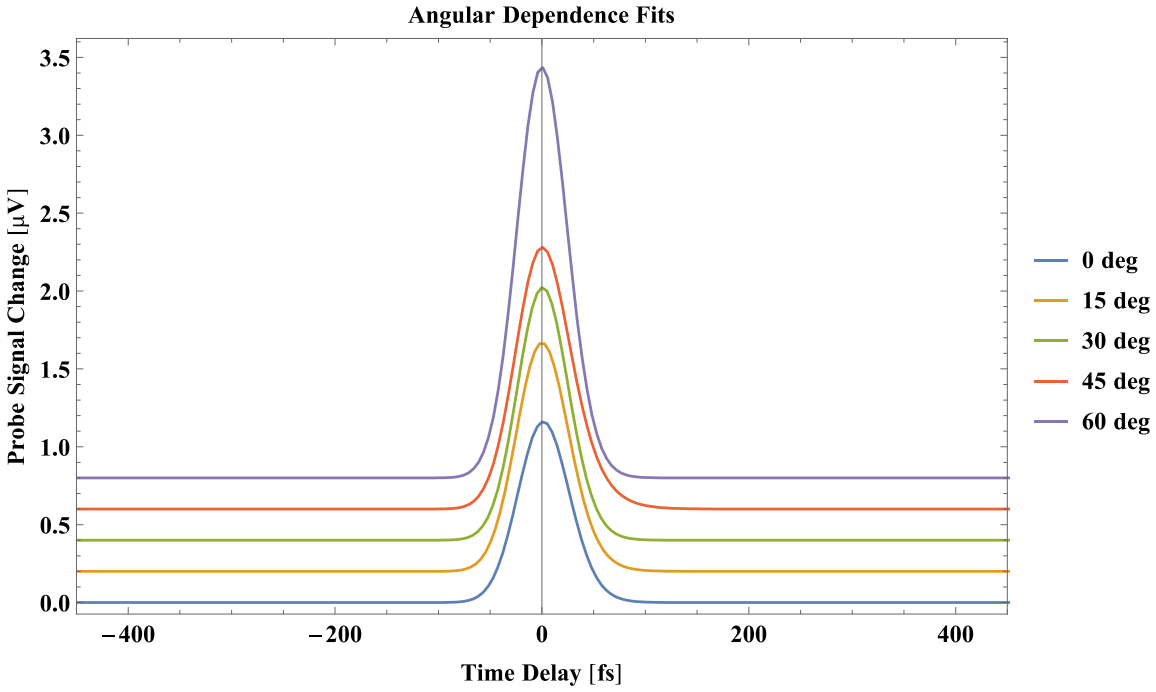

Figure 9. Fits for each pump incident angle data set (note that the background constant, c_0, have been modified to offset each of the scans from each other)

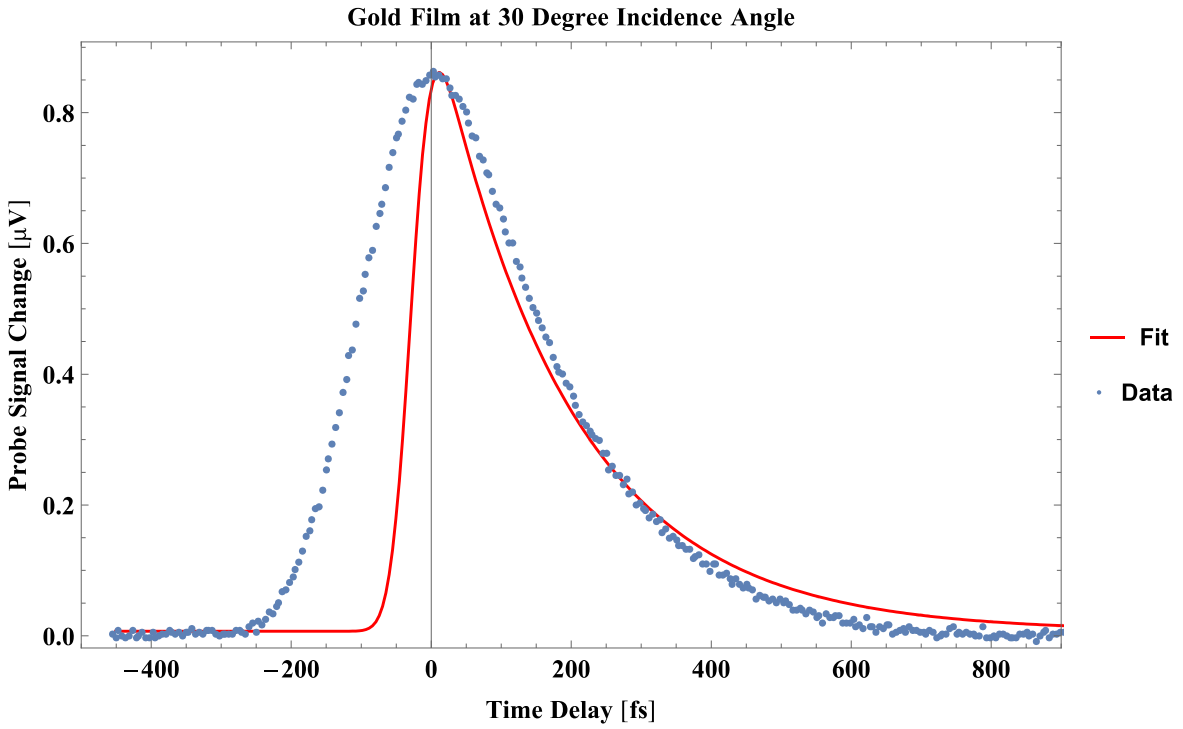

Figure 10. Gold scan and fit for 30 degree pump incidence angle

Incident Angle (degrees)	0	15	30 (ITO)	30 (Gold)	45	60
background c_0 (μV)	0.095	0.121	0.342	0.007	0.087	0.282
Peak amplitude c_1 (μV)	0.076	0.086	0.113	0.015	0.079	0.197
Thermalization time a (fs)	11	13	10	200	18	9

Table 1. Fit parameters for ITO and gold